Original Research Article

JABFM Journal of Applied Biomaterials & Functional Materials

Flexural properties, bond ability, and crystallographic phase of highly translucent multi-layered zirconia

Journal of Applied Biomaterials & Functional Materials
Volume 18: 1–9

DOI: 10.1177/2280800020942717
journals.sagepub.com/home/jbf
SAGE

Yukinori Maruo[1], Kumiko Yoshihara[2], Masao Irie[3], Goro Nishigawa[1], Noriyuki Nagaoka[4], Takuya Matsumoto[3] and Shogo Minagi[4]

Abstract

This study investigated the mechanical properties, bond ability, and crystallographic forms of different sites in a highly translucent, multi-layered zirconia disk. Flexural properties, bond ability to resin cement, and phase composition were investigated at three sites of a highly translucent, multi-layered zirconia disk: incisal, middle, and cervical. Flexural strength (FS) and flexural modulus (FM) were measured with static three-point flexural test. Shear bond strength (SB) to resin cement was measured after 24 h storage (37°C). Phase composition under mechanical stress was analyzed using X-ray diffraction. Without air abrasion, FS at the incisal site yielded the lowest value and was significantly lower than the middle and cervical sites. Air abrasion lowered the FS of each site. FM at the incisal site without air abrasion showed the significantly lowest value, and air abrasion increased its FM value. At the middle and cervical sites, their FM values were higher than the incisal site but were not significantly affected by air abrasion. SB value did not show significant differences among the sites. After sintering, cubic zirconia was detected at each site. Rhombohedral phase transformation occurred after mirror polishing. In highly translucent, multi-layered zirconia which was mainly composed of cubic zirconia, rhombohedral phase transformation occurred under mechanical stress and resulted in weakened mechanical properties.

Keywords

Flexural strength, bond strength, crystallographic phase, zirconia

Date received: 2 April 2020; revised: 15 June 2020; accepted: 17 June 2020

Introduction

Dental alloys restrict light transmission, resulting in reduced ability to mimic the natural appearance of tooth structures. Dental ceramics, on the other hand, score highly on light transmittance. Taking into account other advantages such as superior aesthetics, mechanical properties and biocompatibility, ceramic restorations have enjoyed extensive applications in the dental field.[1–3] Fabricated by computer-aided design/computer-aided machining technology, tetragonal zirconia stabilized by 3 mol% yttrium is a highly aesthetic material which possesses outstanding fracture toughness and mechanical strength for porcelain

[1]Department of Occlusion and Removable Prosthodontics, Okayama University, Okayama, Japan
[2]National Institute of Advanced Industrial Science and Technology, Health Research Institute, Takamatsu, Kagawa, Japan
[3]Department of Biomaterials, Okayama University, Okayama, Japan
[4]Advanced Research Center for Oral and Craniofacial Sciences, Okayama University, Okayama, Japan

Corresponding author:
Dr Yukinori Maruo, Department of Occlusion and Removable Prosthodontics, Okayama University, 2-5-1 Shikata-cho, Okayama, 700-8525, Japan.
Email: ykmar@md.okayama-u.ac.jp

fusion.[4] Thus, the range of applications for zirconia has expanded from conventional full-coverage crowns to resin-bonded fixed apparatus or cantilever restorations such as Rochette or Maryland bridge.[1–2,5,6]

Three crystallographic forms of pure zirconia exist at atmospheric pressure. The monoclinic form is stable at room temperature, the tetragonal form is stable between 1170 and 2370°C, and the cubic form at a higher temperature from 2370 to 2680°C.[4] Polymorphic transformation is induced between tetragonal and monoclinic phases when a mechanical stress is applied.[3] During tetragonal to monoclinic phase transformation, the volume of zirconia expands by about 4%. Alongside this volume expansion is a phenomenon known as transformation toughening, which provides shielding to the crack tip[7,8] and brings about high mechanical properties.[5] Surface damage caused by stress-induced phase transformation includes surface roughness and microcrack formation,[9-11] which reportedly did not affect the mechanical properties and reliability of zirconia because of compensation by volume expansion.

With ceramic-veneered zirconia restorations, there were reported occurrences about chipping of the veneering porcelain or the fracture of zirconia frameworks.[12,13] Although high-strength monolithic zirconia crowns have been introduced for molars to avoid veneer fracture, they are aesthetically inferior to veneered restorations.[12] To circumvent the aesthetic problem of monolithic prostheses, high-translucent zirconia[14] or multi-colored zirconia[15] were developed by increasing the yttria stabilizer content in zirconia. Doping with 5 mol% of yttrium brings about a higher translucency, as well as 50% cubic phase in zirconia, with the latter resulting in markedly decreased fracture toughness and strength.[16] To date, only a few papers on high-translucent zirconia have been published. High-translucent zirconia contains a significantly larger amount of cubic zirconia and a lower amount of alumina. At room temperature, it is difficult for the cubic form to transform to either monoclinic or tetragonal form. In the absence of stress-induced phase transformation, high-translucent zirconia would have reduced mechanical properties and lowered bond strength to resin cements.[17-19]

Establishing a strong and stable bond between zirconia and abutments is crucial for the dispersion of mechanical forces associated with daily oral function. Due to the lack of amorphous silica in zirconia, conventional surface treatments used to enhance the bond strength of glass-containing ceramics—such as hydrofluoric acid etching and salinization—are incapable of creating adequate roughness, micromechanical interlocking, and chemical bonding to zirconia.[20-23] Air abrasion with alumina particles has been used to create a micro-retentive surface on partially stabilized zirconia.[24,25] However, stress-generating surface treatments have been shown to alter the structural stability of zirconia that consists primarily of the cubic form, increase their susceptibility to long-term degradation, and promote cracks and damage in the subsurface zone.

A multi-layered zirconia disk is composed of several layers of cubic-phase zirconia and alumina. The composition varies according to the site from the incisal edge to the cervical side, thus offering monolithic prostheses with high aesthetic and translucent properties. Correspondingly too, the mechanical properties and bond ability to resin cements vary according to the site in a multi-layered disk due to the varied compositions at each site. The aims of this study were to investigate the following on the crystallographic characteristics of highly translucent, multi-layered zirconia which consisted of a significant amount of cubic zirconia: (a) effect of air abrasion on flexural properties and shear bond strength; and (b) influence of mechanical stress triggered by polishing and air abrasion.

The null hypotheses tested in this study were: (a) air abrasion would not affect the flexural properties and bond ability to resin cement of highly translucent zirconia; and (b) there would be no differences in the crystallographic characteristics of highly translucent zirconia among the sintered, polished, and air-abraded conditions.

Methods

Specimen preparation

Presintered, highly translucent, multi-layered zirconia disk (KATANA UTML, Kuraray Noritake Dental, Tokyo, Japan; Table 1) was used to prepare the specimens in this study. Each UTML zirconia disk was sliced into three sites: incisal, middle, and cervical (Figure 1).

For X-ray diffraction (XRD) analysis and shear bond strength test, square disks (approximately 15×15×2 mm) were prepared using a semi-automated, high-speed diamond saw (Accutom, Struers). The surfaces were ground and polished using a 15-μm diamond lapping film to achieve mirror-polished surfaces, and then sintered.

For flexural test, bar-shaped samples of enlarged dimensions (2.5×2.5×31 mm) were cut out from the UTML zirconia disk to compensate for sintering shrinkage (Figures 1). They were then mirror-polished with silicone carbide abrasive paper (P2000, Struers A/S, Rodovre, Denmark) before being sintered in a programmable furnace to obtain the test specimens of 2×2×25 mm.

For shear bond strength test, square samples (approximately 15 mm on a side and 3 mm in thickness) were sliced out from the disk (Figure 1). Each specimen was embedded in a clear acrylic resin cylinder, and the surface of each specimen was mirror-polished with P2000 silicon carbide abrasive paper under water irrigation to eliminate mechanical interlocking engaging force.

Using a grit blaster (Hi-Blaster III, Shofu, Kyoto, Japan) whose nozzle was positioned at 5 mm from the specimen surface, airborne particle abrasion with 50-μm aluminum oxide particles (Al_2O_3; Perlablast® micro, Bego, Bremen, Germany) was carried out at a pressure of 2.8 MPa for 10 s.

Table 1. Materials used in the study.

Materials	Ingredients	Lot	Manufacturer
Zirconia	KATANA™ Zirconia multi-layered disc (A2, 98.5 in diameter, 18 mm in height); $ZrO_2 + Y_2O_3 > 98.0$ (wt%), the others $\leqslant 2.0$ (wt%)	DLMNU	Kuraray Noritake Dental (Tokyo, Japan)
Air abrasion	50-μm aluminum oxide particles (Al_2O_3; Perlablast® micro) Grit blaster (Hi-Blaster III)		Bego, Bremen, Germany Shofu, Kyoto, Japan
Primer	Clearfil Ceramic Primer Ethanol (>80%), 3-trimethoxysilylpropyl methacrylate (< 5%), 10-Methacryloyloxydecyl dihydrogen phosphate	350006	Kuraray Noritake Dental (Tokyo, Japan)
Resin cement	PANAVIA SA Cement Clearfil Esthetic Cement Plus Automix (Universal); A paste: Bis-GMA, TEGDMA, dimethacrylate, 10-MDP, silanized Ba glass filler, silanized colloidal silica, photo-initiator, chemical-initiator B paste: Bis-GMA, dimethacrylate, silanized Ba glass filler, silanized colloidal silica, silanized NaF, chemical accelerator, pigment	CG0077	Kuraray Noritake Dental (Tokyo, Japan)

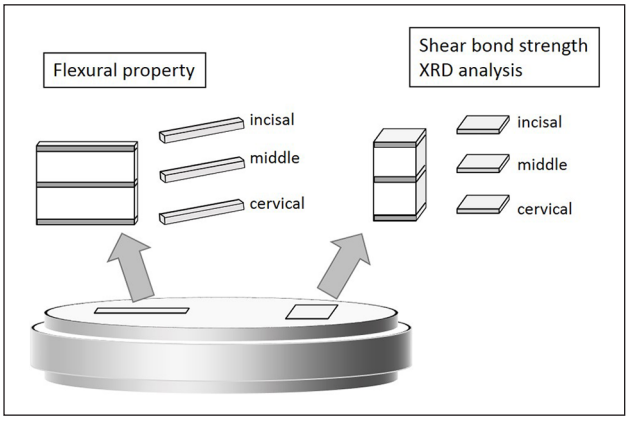

Figure 1. Schematic illustration of specimens prepared from a UTML zirconia disk.

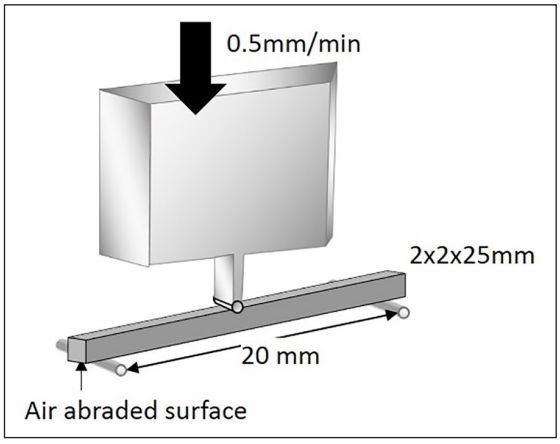

Figure 2. Schematic illustration of flexural strength test. With air-abraded surface placed at the bottom in mounting test jig, flexural strength was measured using a three-point bending technique with a 20-mm span and a crosshead speed of 0.5 mm/min.

XRD analysis

For each site, specimens of four surface conditions were prepared: as-sintered, air abrasion, mirror polishing, or mirror polishing followed by air abrasion. Mirror-polished surfaces were obtained with silicone carbide abrasive paper (P2000, Struers A/S, Rodovre, Denmark).

Crystal phase identification were carried out using an X-ray powder diffractometer (CuKα1 radiation, λ=1.5406 Å; RINT 2500, Rigaku, Tokyo, Japan) operated at 40 kV acceleration, 200 mA current, and a scanning rate of 0.02° s^{-1} for 2θ/θ scans.

Static three-point flexural test

For each site, flexural strength was measured for specimens with and without air abrasion ($n = 10$ for each). Specimens were tested in three-point bending over a 20-mm span at a crosshead speed of 0.5 mm/min (Model 5565, Instron, Norwood, MA, USA), as outlined in ISO 9917-2 (1996) (Figure 2).

One side of the specimens was air-abraded for air abrasion measurement. The air-abraded surface was placed at the bottom in mounting test jig. An external force of maximum 5 kgf (49 N) was applied to its midsection until fracture occurred. Flexural strength and flexural modulus were automatically calculated using a bundled software (Series IX, Instron). Flexural strength, σ, was calculated using the following formula:

$$\sigma = \left(3PL\right) / \left(2bd^2\right)$$

where P is the maximum load at fracture point, L is the distance between supports, b is specimen width, and d is specimen height.

Flexural modulus, E, was calculated as follows:

$$E = \left(P_1 L^3\right) / \left(4bd^3\delta\right)$$

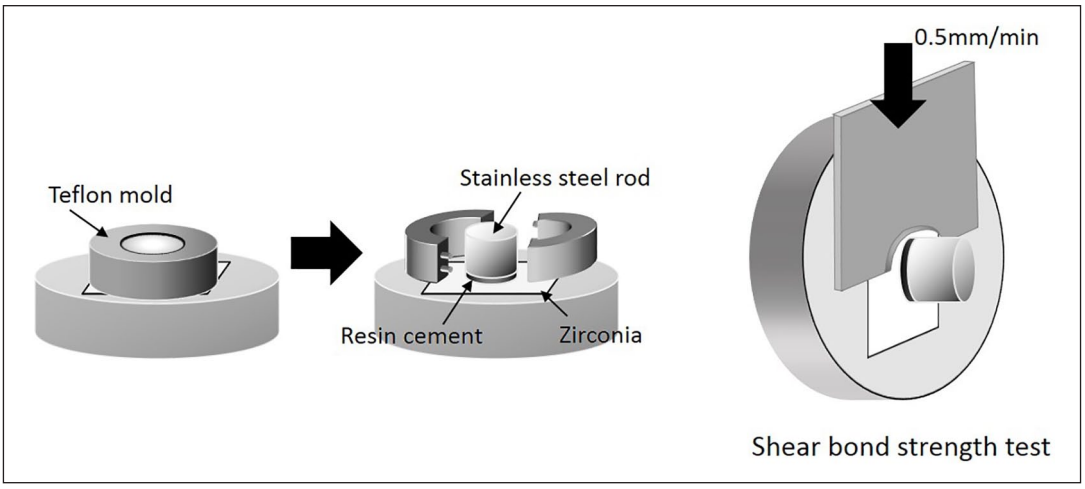

Figure 3. Schematic illustration of shear bond strength test. A stainless steel rod was cemented onto zirconia surface with a Teflon jig mold. Shear bond strength between zirconia surface and resin cement was measured using a universal testing machine with a crosshead speed of 0.5 mm/min.

where E is the flexural modulus, P_1 is the load at an intersection point within the elastic region of stress–strain curve, l is the distance between supports, b is specimen width, d is specimen height, and δ is specimen deformation at P_1.

Among the sites, data of flexural test results were statistically compared using two-way analysis of variance (ANOVA) and Tukey's test, with a 5% limit of error ($p<0.05$) using IBM SPSS Statistics (version 19).

Shear bond strength test

For each site, specimens were randomly assigned into four surface treatment groups comprising a combination of air abrasion and primer pretreatment ($n = 10$ for each). After grit blasting, specimen surfaces were ultrasonically cleaned for 2 min followed by drying with an air stream. A primer agent (Clearfil Ceramic Primer, Kuraray Noritake Dental Inc.) was applied in a thin layer to the entire specimen surface using a disposable sponge. After a gentle blow-dry with oil-free air, a stainless steel rod (3.6 mm diameter, 2.0 mm height) was cemented onto each treated surface using an auto-mixed, dual-cure, self-adhesive resin cement (PANAVIA SA Cement, Kuraray Noritake Dental Inc.) (Figure 3). Cementation was carried out using a Teflon mold jig, where a 10 N load was applied and maintained for 3 min. Bonded specimens were light-cured from two opposite sides for 20 s each. All bonded specimens were immersed in distilled water (37±2°C) for 24 h before shear strength testing. Each specimen was placed in a shear test fixture, and shear bond strength was measured using a universal testing machine (Autograph AG-X, Shimadzu, Kyoto, Japan) at a crosshead speed of 0.5 mm/min. After debonding, the fractured surfaces of zirconia specimens were examined under a light microscope. Failure caused by shear fracture was classified into one of the following three types: (a) adhesive failure between resin cement and zirconia; (b) cohesive failure within resin cement; or (c) mixed-mode failure (adhesive–cohesive).

Among the surface conditions and sites, data were statistically compared using two-way ANOVA and Tukey's test, with a 5% limit of error ($p<0.05$) using IBM SPSS Statistics (version 19).

Results

XRD analysis

For each surface condition, Figures 4 and 5 show the representative XRD patterns of the phase composition of each site. The as-sintered condition showed clear peaks of c-ZrO_2 (200) and t-ZrO_2 (002) (110). Mechanical stress, such as mirror polishing or air abrasion, caused the peaks to shift to a lower angle. The peak on 30° 2θ showed a broadened (101) and a lower tetragonal peak which expressed the rhombohedral ZrO_2 (r-ZrO_2). For each site, the diffraction patterns were affected by the mechanical stress of mirror polishing or air abrasion on the surface.

Static three-point flexural test

Flexural strength results are shown in Tables 2 and 3, and flexural modulus results are shown in Tables 4 and 5. Flexural strength of incisal site without air abrasion showed the lowest value (457.1±82.9 MPa) and was significantly lower than the middle (642.7±68.2 MPa) and cervical (602.0±74.3 MPa) sites ($p<0.05$). Air abrasion significantly lowered the flexural strength values of the middle and cervical sites than without air abrasion.

Flexural modulus of incisal site without air abrasion showed the significantly lowest value (143.3±17.0 GPa,

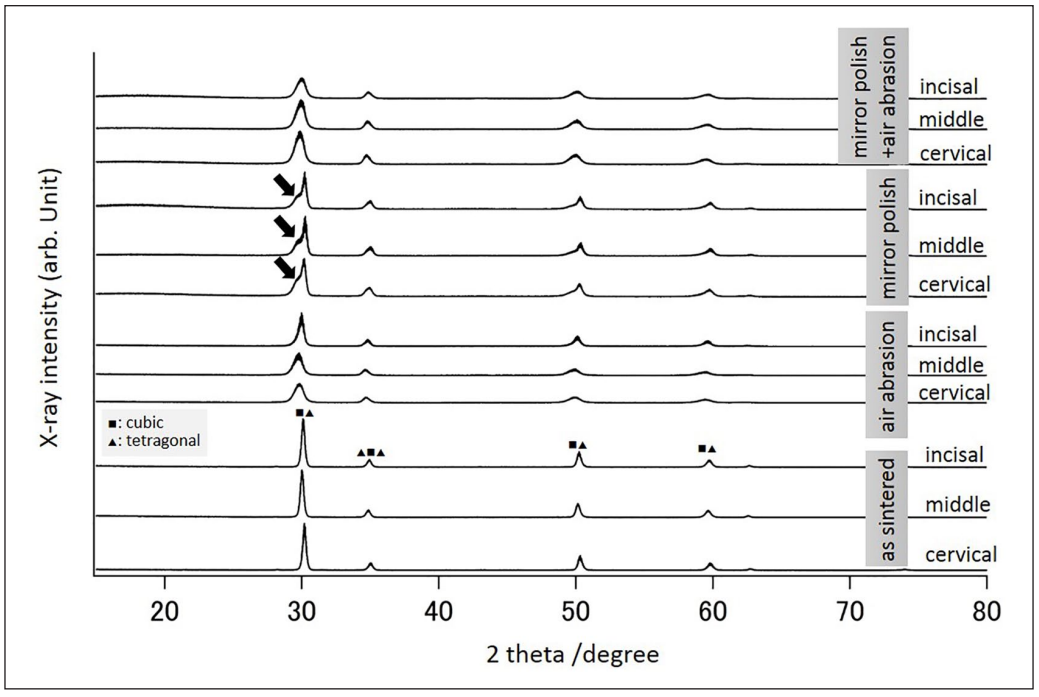

Figure 4. Representative XRD patterns of each site according to surface treatment. Clear c-ZrO_2(200) and t-ZrO_2(002),(110) peaks seen in the as-sintered condition became broadened (101) tetragonal peak in both air-abraded alone and mirror-polish-followed-by-air-abrasion conditions, and rhombohedral ZrO_2 was detected after mirror polishing (black arrows).

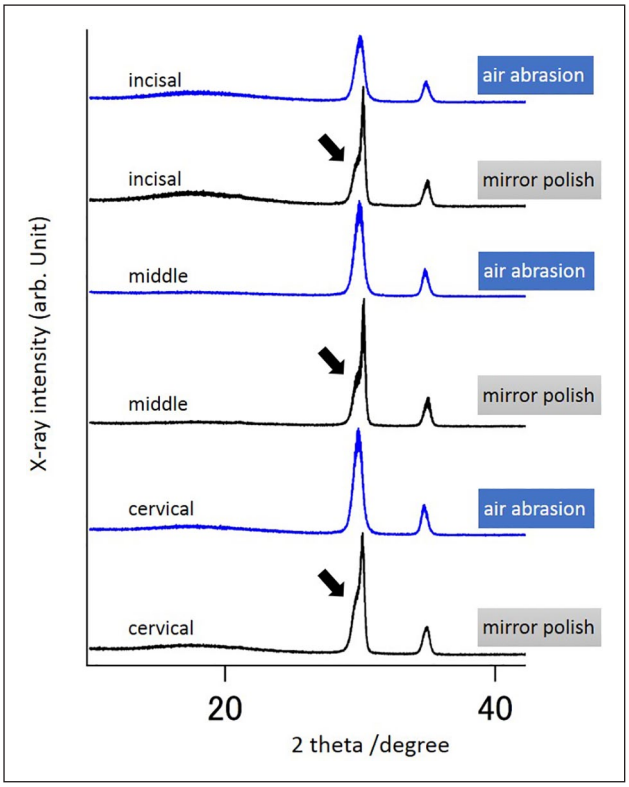

Figure 5. Representative XRD enlarged pattern for the detail of rhombohedral ZrO_2 (black arrows) which were presented in Figure 4.

$p<0.05$). At the middle and cervical sites, the flexural modulus values approximately ranged from 189.5 to 196.5 GPa, which were higher than the incisal site. Air abrasion tended to increase the flexural modulus values, but with no significant effect.

Shear bond strength test

Table 6 and 7 and Figure 5 and 6 show the shear bond strength results and distribution of failure modes after debonding, respectively. Air abrasion significantly increased the shear bond strength value between each site and resin cement ($p<0.05$), and decreased adhesive failure incidence. In contrast, primer pretreatment did not increase the shear strength value at any site.

At the incisal site, ceramic primer pretreatment alone yielded the significantly lowest value (25.3±8.3 MPa, $p<0.05$). Air abrasion significantly increased the shear bond strength value (44.7±8.7 MPa, $p<0.05$), rendering it the highest among all the groups ($p<0.05$).

Unlike the incisal site, air abrasion or ceramic primer pretreatment tended to increase the shear bond strength at both the middle and cervical sites.

Discussion

We hypothesized that air abrasion did not affect the flexural properties and bond ability to resin cement of highly

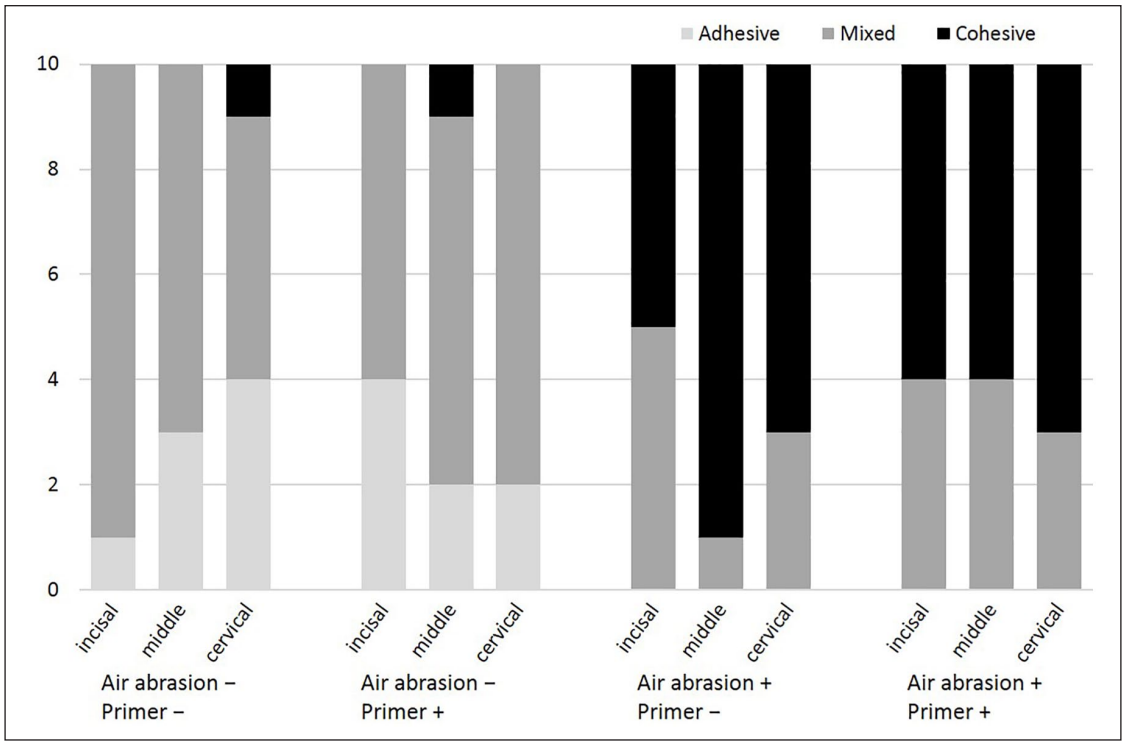

Figure 6. Distribution of failure modes after debonding.

Table 2. The results of 2-way ANOVA of flexural strength.

Source	Type III Sum of Squares	df	Mean Square	F	Sig.	Partial Eta Square	Noncent. Parameter	Observed Power[b]
Corrected model	460676.161[a]	5	92135.232	20.200	.000	.652	100.998	1.000
Intercept	15328478.881	1	15328478.881	3360.583	.000	.984	3360.583	1.000
Air abrasion	229067.888	1	229067.888	50.220	.000	.482	50.220	1.000
Site	173796.307	2	86898.153	19.051	.000	.414	38.103	1.000
Air abrasion×Site	57811.966	2	28905.983	6.337	.003	.190	12.675	.883
Error	246307.827	54	4561.256					
Total	16035462.870	60						
Corrected total	706983.988	59						

[a]*R* squared = .652 (Adjusted *R* Squared = .619).
[b]Computed using alpha = .05.

Table 3. Mean values (SD) of flexural strength (MPa) with and without air abrasion using Al_2O_3 particles. Values with same superscript letters (a–c) in each column are not significantly different ($p>0.05$).

Group	Site		
Air abrasion	Incisal	Middle	Cervical
–	457.1 (82.9)[ab]	642.7 (68.2)[c]	602.0 (74.3)[c]
+	401.8 (41.6)[a]	437.2 (34.2)[ab]	491.9 (86.2)[b]

translucent zirconia; and there were no differences in the crystallographic characteristics of highly translucent zirconia among the sintered, polished, and air-abraded conditions. The ANOVA analysis in this study revealed that air abrasion had an influence on flexural strength and shear bond strength ($p<0.001$), but not on flexural modulus. Although the shear bond strength value did not depend on the site difference in the zirconia disk, the flexural properties significantly depended on the site difference ($p<0.001$). Mechanical stress through mirror polishing to the zirconia detected the rhombohedral phase transformation. The null hypotheses on the flexural strength, the shear bond strength, and the crystallographic characteristics were rejected.

Under the as-sintered control condition in this study, the incisal site, which presents the highest translucency, showed significantly lower flexural strength and modulus

Table 4. The results of 2-way ANOVA of flexural modulus.

Source	Type III Sum of Squares	df	Mean Square	F	Sig.	Partial Eta Square	Noncent. Parameter	Observed Power[b]
Corrected model	22775.629[a]	5	4555.126	7.375	.000	.406	36.876	.998
Intercept	1950629.643	1	1950629.643	3158.235	.000	.983	3158.235	1.000
Air abrasion	2006.817	1	2006.817	3.249	.077	.057	3.249	.425
Site	19856.682	2	9928.341	16.075	.000	.373	32.150	.999
Air abrasion×Site	912.130	2	456.065	.738	.483	.027	1.477	.169
Error	33352.168	54	617.633					
Total	2006757.440	60						
Corrected total	56127.797	59						

[a]*R* squared = .406 (Adjusted *R* Squared = .351).
[b]Computed using alpha = .05.

Table 5. Mean values (SD) of flexural modulus (GPa) with and without air abrasion using Al_2O_3 particles. Values with same superscript letters (a, b) in each column are not significantly different ($p>0.05$).

Group	Site		
Air abrasion	Incisal	Middle	Cervical
–	143.3 (17.0)[a]	190.8 (23.2)[b]	189.5 (14.6)[b]
+	165.9 (28.4)[ab]	195.9 (34.2)[b]	196.5 (18.0)[b]

than the middle and cervical sites. Air abrasion decreased the flexural strength at each site; nonetheless, the cervical site retained a higher strength value than the incisal site. While the high translucency of zirconia could be obtained from a larger grain size and an increased amount of cubic phase, the latter caused the transformation rate from tetragonal to monoclinic phase to decrease, and eventually deteriorated the fracture toughness of highly translucent zirconia ceramics.

With the highly translucent zirconia used in this study, XRD analysis captured the extremely slight differences in phase composition among the three sites. Through the different surface treatments, XRD analysis revealed similar effects on phase composition among the three sites. In higher-translucent zirconia, the tetragonal phase could be over-stabilized, resulting in poor transformability under mechanical stress.[26] As for the effects of different surface treatments on the flexural properties of different sites, this study did not yield clear results.

Without air abrasion, the shear bond strength of the incisal site did not benefit from the ceramic primer which contained the silane coupling agent and 10-MDP, thus yielding the lowest shear bond strength value. Air abrasion increased the shear bond strength of all the three sites. When treated in conjunction with the ceramic primer, the latter did not synergistically enhance the shear bond strength of the middle and cervical sites. However, shear bond strength of the incisal site deteriorated with primer pretreatment. Indeed, the incisal site—which presents the highest translucency—exhibited different bond strength behaviors when compared with the middle and cervical sites.

The shear bond strength results of different sites in this study when subject to air abrasion and adhesive primer treatments revealed that lower mechanical properties were related to these two factors: larger grain size[27] and the vulnerability of micro-retentive surface produced by air abrasion.[17,18] Increase in cubic phase would diminish the stress-induced transformation toughening of zirconia. Although air abrasion would adversely affect mechanical properties because of the microcracks it produced on the adhesive surface, the higher bond ability between the highly translucent zirconia and resin cement compensated for the deteriorated mechanical properties.

It has been reported that when mechanical stress such as fine polishing or grinding was applied, phase transformation of partially stabilized zirconia occurred at a depth of 4 μm from the surface.[4] Tetragonal to monoclinic phase transformation is accompanied by a 4% volume expansion, which shields the microcrack from applied stress[7,8] and eventually brings about high mechanical properties.[3,5] Instead of tetragonal to monoclinic phase transformation, XRD patterns in this study showed that air abrasion made the clear peak broaden and mirror polishing led to rhombohedral phase formation. The mechanical stress of mirror polishing and air abrasion could induce phase transformation, and thus the transformation to rhombohedral phase in highly translucent zirconia in this study. Therefore, the weakened mechanical properties observed in this study could be attributed to rhombohedral phase transformation.

XRD experiments on various cut, abraded, and polished zirconia ceramic surfaces have identified the rhombohedral phase with a maximum intensity (111)r peak at $2\theta = 29.8°$.[28] It has been reported that rhombohedral zirconia was detected on the abraded surfaces of partially stabilized zirconia, and that this phase was detected at all levels of grinding and for various amounts of yttria dopant, even in the fully stabilized cubic zirconia.[4] Chemical etching could reduce the rhombohedral phase and increase the monoclinic phase. Therefore, it was suggested that the rhombohedral phase is an intermediate in

Table 6. The results of 3-way ANOVA of shear bond strength.

Source	Type III Sum of Squares	df	Mean Square	F	Sig.	Partial Eta Square	Noncent. Parameter	Observed Power[b]
Corrected model	5183.216[a]	11	471.201	6.914	.000	.413	76.055	1.000
Intercept	155091.385	1	155091.385	2275.719	.000	.955	2275.719	1.000
Air abrasion	4035.623	1	4035.623	59.216	.000	.354	59.216	1.000
Primer	62.555	1	62.555	.918	.340	.008	.918	.158
Site	318.020	2	159.010	2.333	.102	.041	4.666	.464
Air abrasion×Primer	55.192	1	55.192	.810	.370	.007	.810	.145
Air abrasion×Site	375.462	2	187.731	2.755	.068	.049	5.509	.533
Primer×Site	332.992	2	166.496	2.443	.092	.043	4.886	.482
Air abrasion×Primer×Site	3.372	2	1.686	0.25	.976	.000	.049	.054
Error	7360.255	108	68.151					
Total	167634.855	120						
Corrected total	12543.470	119						

[a]*R* squared = .413 (Adjusted *R* Squared = .353).
[b]Computed using alpha = .05.

Table 7. Mean values (SD) of shear bond strength (MPa) of all pretreatment groups. Values with same superscript letters (a–d) in each column are not significantly different ($p>0.05$).

Group		Site		
Air abrasion	Primer	Incisal	Middle	Cervical
–	–	26.4 (6.7)[ab]	27.7 (7.7)[ab]	32.1 (9.6)[abc]
–	+	25.3 (8.4)[a]	34.5 (7.2)[abcd]	34.9 (7.7)[abcd]
+	–	44.7 (8.7)[d]	38.3 (9.1)[bcd]	42.2 (6.0)[cd]
+	+	40.2 (9.1)[cd]	42.0 (9.7)[cd]	43.2 (8.3)[cd]

the tetragonal to monoclinic transformation and a barrier to further tetragonal transformation.[28] It was also reported that the rhombohedral phase could be removed by annealing at 1000°C and that the powder removed by grinding contained no rhombohedral phase.[4] This means that rhombohedral phase could exist only in the presence of stress, such as that introduced by polishing or grinding.[28]

The flexural properties were determined with the three-point bending test, which is more unpredictable as it depends on many factors including sample size, shape, and surface conditions. The shear bond strength between the zirconia and resin cement was also estimated according to ISO 29022, because the test is required to shear off the zirconia surface from the resin cement parallel to the bonding interface. But the shrinkage of resin cements, which occurs always during polymerization on the test surface, is not considered in this test design. Those in vitro measures are, however, assumed to be one of the most commonly used and applied for the regulatory approval of dental materials. Because this study investigated the initial findings either of bond strength between zirconia and resin cement or flexural properties of the zirconia, the long-term durability for bonding strength or effects for the exposure of air abrasion remained still unclear.

Conclusions

Within the limitations of this study, the following conclusions were drawn:

(1) Highly translucent, multi-layered zirconia was mainly composed of cubic zirconia. Weakened mechanical properties were attributed to rhombohedral phase transformation, which occurred under mechanical stress.
(2) Air abrasion produced microcracks on the adhesive surface, thereby compromising the mechanical properties. However, air abrasion also resulted in higher bond ability between highly translucent zirconia and resin cements, thereby compensating for the deteriorated mechanical properties.

Declaration of conflicting interests

The authors declared no potential conflicts of interest with respect to the research, authorship, and/or publication of this article.

Funding

The authors disclosed receipt of the following financial support for the research, authorship, and/or publication of this article: This work was partially supported by a Grant-in-aid for Scientific Research (KAKENHI), Grant Number 18K09681, from the Japan Society for the Promotion of Science (JSPS).

ORCID iD

Yukinori Maruo https://orcid.org/0000-0001-9434-0978

References

1. Tinschert J, Zwez D, Marx R, et al. Structural reliability of alumina-, feldspar-, leucite-, mica-, and zirconia-based ceramics. *J Dent* 2000; 28: 529–535.

2. Guazzato M, Albakry M, Ringer SP, et al. Strength, fracture toughness and microstructure of a selection of all-ceramic materials, Part I. Pressable and alumina glass-infiltrated ceramics. *Dent Mater* 2004; 20: 441–448.
3. Lazar DR, Bottino MC, Ozcan M, et al. Y-TZP ceramic processing from coprecipitated powders: A comparative study with three commercial dental ceramics. *Dent Mater* 2008; 24: 1676–1685.
4. Denry I.L and Holloway JA. Microstructural and crystallographic surface changes after grinding zirconia-based dental ceramics. *J Biomed Mater Res B Appl Biomater* 2006; 76: 440–448.
5. Piconi C and Maccauro G. Zirconia as a ceramic biomaterial. *Biomaterials* 1999; 20: 1–25.
6. Stylianou A, Liu PR, O'Neal SJ, et al. Restoring congenitally missing maxillary lateral incisors using zirconia-based resin bonded prostheses. *J Esthet Restor Dent* 2016; 28: 8–17.
7. Kelly JR and Denry I. Stabilized zirconia as a structural ceramic: An overview. *Dent Mater* 2008; 24: 289–298.
8. Vichi A, Sedda M, Fabian Fonzar R, et al. Comparison of contrast ratio, translucency parameter, and flexural strength of traditional and "augmented translucency" zirconia for CEREC CAD/CAM system. *J Esthet Restor Dent* 2016; 28: S32–S39.
9. Kosmac T, Oblak C, Jevnikar P, et al The effect of surface grinding and sandblasting on flexural strength and reliability of Y-TZP zirconia ceramic. *Dent Mater* 1999; 15: 426–433.
10. Kosmac T, Oblak C, Jevnikar P, et al. Strength and reliability of surface treated Y-TZP dental ceramics. *J Biomed Mater Res* 2000; 53: 304–313.
11. Luthardt RG, Holzhüter M, Sandkuhl O, et al. Reliability and properties of ground Y-TZP-zirconia ceramics. *J Dent Res* 2002; 81: 487–491.
12. Johansson C, Kmet G, Rivera J, et al. Fracture strength of monolithic all-ceramic crowns made of high translucent yttrium oxide-stabilized zirconium dioxide compared to porcelain-veneered crowns and lithium disilicate crowns. *Acta Odontol Scand* 2014; 72: 145–153.
13. Abdulmajeed AA, Donovan TE, Cooper LF, et al. Fracture of layered zirconia restorations at 5 years: A dental laboratory survey. *J Prosthet Dent* 2017; 118: 353–356.
14. Flinn BD, Raigrodski AJ, Mancl LA, et al. Influence of aging on flexural strength of translucent zirconia for monolithic restorations. *J Prosthet Dent* 2017; 117: 303–309.
15. Ueda K, Güth JF, Erdelt K, et al. Light transmittance by a multi-colored zirconia material. *Dent Mater J* 2015; 34: 310–314.
16. Zhang F, Inokoshi M, Batuk M, et al. Strength, toughness and aging stability of highly-translucent Y-TZP ceramics for dental restorations. *Dent Mater* 2016; 32: e327–e337.
17. Inokoshi M, Vanmeensel K, Zhang F, et al. Aging resistance of surface-treated dental zirconia. *Dent Mater* 2015; 31: 182–194.
18. Aurelio IL, Marchionatti AM, Montagner AF, et al. Does air particle abrasion affect the flexural strength and phase transformation of Y-TZP? A systematic review and meta-analysis. *Dent Mater* 2016; 32: 827–845.
19. Inokoshi M, Shimizu H, Nozaki K, et al. Crystallographic and morphological analysis of sandblasted highly translucent dental zirconia. *Dent Mater* 2018; 34: 508–518.
20. Aboushelib MN, Feilzer AJ and Kleverlaan CJ. Bonding to zirconia using a new surface treatment. *J Prosthodont* 2010; 19: 340–346.
21. Casucci A, Goracci C, Chieffi N, et al. Microtensile bond strength evaluation of self-adhesive resin cement to zirconia ceramic after different pre-treatments. *Am J Dent* 2012; 25: 269–275.
22. Quinn GD, Studart AR, Hebert C, et al. Fatigue of zirconia and dental bridge geometry: Design implications. *Dent Mater* 2010; 26: 1133–1136.
23. Salem R, Naggar GE, Aboushelib M, et al. Microtensile bond strength of resin-bonded high-translucency zirconia using different surface treatments. *J Adhes Dent* 2016; 18: 191–196.
24. Inokoshi M, De Munck J, Minakuchi S, et al. Meta-analysis of bonding effectiveness to zirconia ceramics. *J Dent Res* 2014; 93: 329–334.
25. Okada M, Taketa H, Torii Y, et al. Optimal sandblasting conditions for conventional-type yttria-stabilized tetragonal zirconia polycrystals. *Dent Mater* 2019; 35: 169–175.
26. Camposilvan E, Leone R, Gremillard L, et al. Aging resistance, mechanical properties and translucency of different yttria-stabilized zirconia ceramics for monolithic dental crown applications. *Dent Mater* 2018; 34: 879–890.
27. Heuer AH, Claussen N, Kriven WM, et al. Stability of tetragonal ZrO_2 particles in ceramic matrices. *J Am Ceram Soc* 1982; 65: 642–650.
28. Burke DP and Rainforth WM. Intermediate rhombohedral (r-ZrO_2) phase formation at the surface of sintered Y-TZP's. *J Mater Sci Lett* 1997; 16: 883–885.